JAM CM Journal of Applied Mathematics and Computational Mechanics 2026, 25(1), 74-85
www.amcm.pcz.pl p-ISSN 2299-9965
DOI: 10.17512/jamcm.2026.1.07 e-ISSN 2353-0588

BENDING OF FUNCTIONALLY GRADED MICRO/NANO PLATES WITH THE FLEXOELECTRIC EFFECT BY THE MOVING FINITE ELEMENT METHOD

Ladislav Sator, Miroslav Repka

Institute of Construction and Architecture, Slovak Academy of Sciences, Bratislava, Slovakia
ladislav.sator@savba.sk, miroslav.repka@savba.sk

Received: 24 September 2025; Accepted: 26 January 2026

Abstract. Micro/nano structural elements are utilized in various branches of engineering practice as parts of MEMS/NEMS sensors and actuators. Therefore, it is necessary to investigate the mechanical behaviour of such structures in the micro/nano scales. It is well known that strain-gradients can induce polarization even in non-piezoelectric solids, and this effect is called as direct flexoelectricity. Besides the direct flexoelectric effect, there exist the converse flexoelectric effect, wherein an applied electric field gradient induces mechanical strains. The paper aims to derive the formulation for bending of flexoelectric FGM micro/nano plates taking into account the assumptions of the Kirchhoff-Love plate bending theory. We shall investigate the influence of the gradation parameters on the static responses of the flexoelectric micro/nano plates. The functional gradation of material coefficients complies with rule of mixture. For the numerical solution of complex boundary value problems, the moving finite element approximation technique is applied for spatial variations of field variables. Several numerical experiments are presented for illustration of multi-physical effects in the bending of flexoelectric FGM plates.

MSC 2010: *74A40, 82D80, 91G60*
Keywords: *thin micro/nano plates, flexoelectricity, functional gradation, moving finite element method*

1. Introduction

Great attention has been paid to the investigation of the mechanical behaviour of beam- and plate-like structural elements in micro- and nano-scale devices due to their widespread utilization in several branches of engineering practice [1-3]. The ongoing miniaturization efforts in micro- and nano-electromechanical systems (MEMS/NEMS) have underscored a deficiency in classical continuum mechanics, specifically its inability to account for observed size-dependent phenomena at reduced scales [4]. Furthermore, at these small scales, the flexoelectric effect – the coupling between mechanical strain gradients and electric polarization – has become increasingly

significant, particularly in centrosymmetric dielectrics where conventional piezoelectricity is absent. This phenomena offers new avenues for smart material design. Therefore, the adoption of higher-grade theories is necessary for the accurate modelling of micro/nanoplates made of such materials.

Nowadays, the laminated composite materials are widely used in the construction of fundamental structural elements. It is well known the discontinuities on interfaces between two layers in such composites lead to concentrations of gradient fields, which is the significant factor of failure of laminated structures. This negative phenomenon of delamination can be overcome by replacing laminated plate structures by functionally graded ones [5, 6], if possible. Therefore, the investigation of the response of functionally graded (FGM) micro/nano plates with a flexoelectric effect has become attractive, which can be confirmed by the relevant number of papers [7-10] on this topic.

This paper presents a theoretical and numerical investigation into the static bending of thin FGM micro/nanoplates. The analysis incorporates in-plane gradation of material coefficients within the framework of the strain gradient theory of elastic media and the Kirchhoff-Love plate theory, explicitly accounting for flexoelectric effects in centrosymmetric dielectric materials. To overcome inaccuracies associated with the approximation of high-order derivatives, the primary governing PDEs are decomposed into a system of second-order PDEs. The numerical implementation utilizes a strong formulation, applying the Moving Finite Element (MFE) approximation method [11]. Through a series of numerical experiments, the study presents the influence of the in-plane gradations of various material coefficients on the physical fields of the FGM micro/nanoplate.

2. Governing equations for thin FGM micro/nano plate

2.1. Constitutive relations

The internal energy of a dielectric material with flexoelectricity depends on strains, strain gradients, and the electric field. For a centrosymmetric dielectric material, the electric enthalpy density H^e can be written as:

$$H^e = \frac{1}{2} c_{ijkl} \varepsilon_{ij} \varepsilon_{kl} - \frac{1}{2} a_{ij} E_i E_j - f_{ijkl} E_i \varepsilon_{jk,l} \tag{1}$$

The first term stands for the elastic strain energy, where c_{ijkl} is the fourth-rank elastic parameter tensor, the second term is the electrical energy, where a_{ij} is the second-rank permittivity tensor, and the third term is the flexoelectric coupling energy, which links the electric field E_i to the strain gradients $\varepsilon_{jk,l}$, where f_{ijkl} is the fourth-rank flexoelectric tensor.

From this enthalpy, we can derive the constitutive relations for the Cauchy stress tensor σ_{ij}, the higher-order stress tensor τ_{ijk}, and the electric displacement vector D_i:

$$\sigma_{ij} = \frac{\partial H^e}{\partial \varepsilon_{ij}} = c_{ijkl}\varepsilon_{kl}$$
$$\tau_{ijk} = \frac{\partial H^e}{\partial \varepsilon_{jk,i}} = -f_{ijkl}E_l$$
$$D_i = -\frac{\partial H^e}{\partial E_i} = a_{ij}E_j + f_{ijkl}\varepsilon_{jk,l} \tag{2}$$

The strain tensor ε_{ij} and the electric field vector E_j are related to the displacements u_i and the electric potential ϕ by

$$\varepsilon_{ij} = \frac{1}{2}\left(u_{i,j} + u_{j,i}\right)$$
$$E_j = -\phi_{,j} \tag{3}$$

The strain-gradient tensor κ_{ijk} is defined as

$$\kappa_{ijk} = \varepsilon_{ij,k} = \frac{1}{2}\left(u_{i,jk} + u_{j,ik}\right) \tag{4}$$

For isotropic materials, the material parameter tensors simplifies as

$$c_{ijkl} = \frac{E\nu}{(1+\nu)(1-2\nu)}\delta_{ij}\delta_{kl} + \frac{E}{2(1+\nu)}(\delta_{ik}\delta_{jl} + \delta_{il}\delta_{jk}),$$
$$f_{ijkl} = f_1(\delta_{il}\delta_{jk} + \delta_{jl}\delta_{ik}) + f_2\delta_{kl}\delta_{ij},$$
$$a_{ij} = a\delta_{ij}, \tag{5}$$

For the elastic parameter, flexoelectric coefficient and permittivity tensor, respectively.

2.2. Governing equations

In the Kirchhoff-Love plate bending theory, the displacements can be expressed in terms of transversal displacements (deflections) w as

$$u_i = -x_3\delta_{i\alpha}w_{,\alpha} + \delta_{i3}w \tag{6}$$

Now, in view of (6), the linear stain tensor becomes

$$\varepsilon_{\alpha\beta} = -x_3 w_{,\alpha\beta},$$
$$\varepsilon_{33} = 0 \tag{7}$$

and strain gradients are

$$\kappa_{\alpha\beta\gamma} = -x_3 w_{,\alpha\beta\gamma}, \ \kappa_{\alpha\beta 3} = -w_{,\alpha\beta} \tag{8}$$

where Greek indices $(\alpha, \beta, \gamma) = 1, 2$, and a comma denotes the partial differentiation. In view of strains (7) and strain gradients (8), we have

$$\begin{aligned}
e_{kk} &= -x_3 w_{,\gamma\gamma} \\
\sigma_{\alpha\beta}(x,z) &= \frac{E}{1-\nu^2}\frac{1-\nu}{H}\left\{-x_3 \tau_{\alpha\beta}^{(w)}(x)\right\}, \\
\sigma_{33}(x,z) &= \frac{E\nu}{1-\nu^2}\frac{1-\nu}{H}\left\{x_3 w_{,\gamma\gamma}\right\}, \\
\tau_{\alpha\beta\gamma} &= f_1(\phi_{,\alpha}\delta_{\beta\gamma} + \phi_{,\beta}\delta_{\alpha\gamma}) + f_2(x_1)\phi_{,\gamma}\delta_{\alpha\beta} \\
\tau_{\alpha\beta 3} &= f_2(x_1)\phi_{,3}\delta_{\alpha\beta} \\
D_\alpha &= -a\phi_{,\alpha} - \left(2f_1 + f_2\right)w_{,\alpha\gamma\gamma} \\
D_3 &= -a\phi_{,3} - f_1 w_{,\gamma\gamma}
\end{aligned} \tag{9}$$

with $\tau_{\alpha\beta}^{(w)} := Hw_{,\alpha\beta} + \nu\delta_{\alpha\beta}w_{,\gamma\gamma}$, where $H = 1-\nu$ due to the applied plane stress formulation.

The governing equations as well as the boundary conditions can be derived from the variational principle

$$\int_\Omega \int_{-h/2}^{h/2} (\sigma_{ij}\delta\varepsilon_{ij} + \tau_{ijk}\delta\varepsilon_{jk,i} + D_k\delta\phi_k) dx_3 d\Omega - \int_\Omega q\delta w d\Omega = 0. \tag{10}$$

Owing to the 3D functional dependence of the electric potential field, the dependence of stresses on the transversal and in-plane coordinates is not factorized. Since $L/h \gg 1$, it is reasonable to assume the power series expansion w.r.t. the dimensionless coordinate $z = x_3/h$ as

$$\phi \approx \psi_0 + z\psi_1 + z^2\psi_2, \tag{11}$$

with ψ_a for $a = 0, 1, 2$, being new field variables. Two of them can be determined from the boundary conditions on the bottom and top surfaces of the plate.

Let us consider a Dirichlet boundary condition on both the bottom and the top surfaces of the plate, respectively. Then we may write

$$\begin{aligned}
&\phi(\mathrm{x}, \pm h/2) = \psi_0 \pm \frac{1}{2}\psi_1 + \left(\frac{1}{2}\right)^2 \psi_2 = \phi^{\pm} \\
&\Rightarrow \psi_1(\mathrm{x},t) = \phi^+ - \phi^-, \quad \psi_2 = 2(\phi^+ + \phi^-) - 4\psi_0
\end{aligned} \tag{12}$$

Then, in view of (12), Eq. (11) results into

$$\phi \approx \left(1-4z^2\right)\psi_0 + z\Phi^- + 2z^2\Phi^+, \tag{13}$$

where $\Phi^{\pm} = \phi^+ \pm \phi^-$.

Hence,

$$\phi_{,k} = \left[\left(1-4z^2\right)\psi_{0,\alpha} + z\Phi^-_{,\alpha} + 2z^2\Phi^+_{,\alpha}\right]\delta_{k\alpha} + \frac{1}{h}\left[-8z\psi_0 + \Phi^- + 4z\Phi^+\right]\delta_{k3} \tag{14}$$

After substituting Eq. (14) into (10), we obtain

$$\int_{\Omega}\left\{-M_{\alpha\beta}\delta w_{,\alpha\beta} - M_{\alpha\beta\gamma,\alpha\beta\gamma}\delta w_{,\alpha\beta\gamma} - R_{\alpha\beta}\delta w_{,\alpha\beta} + B_{\alpha}\delta\psi_{0,\alpha} + B_3\delta\psi_0\right\}d\Omega \tag{15}$$

where semi-integral fields are defined as

$$M_{\alpha\beta} = \int_{-h/2}^{h/2} x_3\sigma_{\alpha\beta}dx_3,\ M_{\alpha\beta\gamma} = \int_{-h/2}^{h/2} x_3\tau_{\alpha\beta\gamma}dx_3,\ R_{\alpha\beta} = \int_{-h/2}^{h/2}\tau_{\alpha\beta 3}dx_3$$
$$B_{\alpha} = \int_{-h/2}^{h/2}\left(1-4\left(\frac{x_3}{h}\right)^2\right)D_{\alpha}dx_3,\ B_3 = -\frac{8}{h}\int_{-h/2}^{h/2}\frac{x_3}{h}D_3dx_3. \tag{16}$$

In linear theories, it is convenient to utilize dimensionless formulations. Let us introduce the dimensionless variables

$$x_{\beta}^{*} := \frac{x_{\beta}}{L},\ x_3^{*} := \frac{x_3}{h_0} = h^{*}(x)z,\ h(x) = h_0h^{*}(x), \tag{17}$$

and the dimensionless fields

$$w^{*} := \frac{w}{h_0},\ \psi_0^{\ *} := \frac{\psi_0}{\Phi_0},\ \Phi^{+*} := \frac{\Phi^+}{\Phi_0},\ \Phi^{-*} := \frac{\Phi^-}{\Phi_0}. \tag{18}$$

In a general sense, the material coefficients in the FGM plate can be dependent on both the transversal as well as in-plane coordinates.

Let us consider the coordinate dependence of Young's modulus, permittivity and flexoelectric coefficients in the factorized form

$$E(\mathbf{x}) = E_0E_H^{*}(\mathbf{x}),$$
$$a(x) = a_0a_H^{*}(\mathbf{x}),$$
$$f_a(\mathbf{x}) = f_0f_{aH}^{*}(\mathbf{x}),\quad a = 1,2 \tag{19}$$

assuming the power-law gradation over the in-plane directions of the plate

$$E_H^*(x_1^*) = 1 + \zeta\left(\frac{x_1^*}{L}\right)^p$$
$$a_H^*(x_1^*) = 1 + \varepsilon\left(\frac{x_1^*}{L}\right)^r$$
$$f(x_1^*) = 1 + \lambda\left(\frac{x_1^*}{L}\right)^s \tag{20}$$

where ζ, ε, λ and p, r, s are the values of the levels and exponents of the power-law gradation, respectively.
Then the governing equations in dimensionless formulation are

$$(M_{\alpha\beta}^* - R_{\alpha\beta}^*)_{,\alpha\beta} - M_{\alpha\beta\gamma,\alpha\beta\gamma}^* = q^*$$
$$B_{\alpha,\alpha}^* - B_3^* = 0 \tag{21}$$

with $q^* = \dfrac{L^4}{D_0 h_0} q_0$.
And the boundary restrictions

$$n_\beta B_\beta \delta\psi_0 = 0$$
$$V^* \delta w^*\Big|_{\partial\Omega_V} = 0, \quad S^* \delta\left(\frac{\partial w^*}{\partial \boldsymbol{n}}\right)\Big|_{\partial\Omega_S} = 0, \quad S^{*(ws)} \delta\left[\frac{\partial}{\partial \boldsymbol{n}}\left(\frac{\partial w^*}{\partial \boldsymbol{n}}\right)\right]\Big|_{\partial\Omega_S} = 0 \tag{22}$$

in which

$$V^* := n_\alpha\left[M_{\alpha\beta,\beta}^* - M_{\alpha\beta\gamma,\beta\gamma}^* + \left(\frac{L}{h_0}\right)^2 R_{\alpha\beta,\beta}^*\right]$$
$$- \sum_c \left[\left[T^*\right]\right]\delta\left(\mathbf{x}^* - \mathbf{x}_c^*\right) + t_\alpha T_{,\alpha}^*$$
$$- \kappa^* \sum_c \left(\left[\left[M^{*(s)}\right]\right]\delta\left(\mathbf{x}^* - \mathbf{x}_c^*\right) + t_\alpha M_{,\alpha}^{*(s)}\right)$$
$$+ \sum_c \left[\left[t_\alpha M_{,\alpha}^{*(wt)}\right]\right]\delta\left(\mathbf{x}^* - \mathbf{x}_c^*\right) + t_\beta\left(t_\alpha M_{,\alpha}^{*(wt)}\right)_{,\beta}$$
$$T^* := t_\alpha n_\beta M_{\alpha\beta}^{*(w)} - M_{\alpha\beta\gamma,\gamma}^* + \left(\frac{L}{h_o}\right)^2 R_{\alpha\beta}^*$$
$$M^{*(s)} := 2 n_\alpha t_\beta n_\gamma M_{\alpha\beta\gamma}, \quad M^{*(wt)} := t_\alpha t_\beta n_\gamma M_{\alpha\beta\gamma}, \quad \kappa^* = n_\alpha t_\beta \frac{\partial t_\alpha}{\partial x_\beta^*}$$

$$S^{*(w)} := -n_\alpha n_\beta \left[M^*_{\alpha\beta} - M^*_{\alpha\beta\gamma,\gamma} + \left(\frac{L}{h_o}\right)^2 R^*_{\alpha\beta} \right]$$
$$- \sum_c [[M^{*(s)}]] \delta(x^* - x^*_c) + t_\alpha M^{*(s)}_\alpha$$
$$+ \kappa^* t_\alpha t_\beta n_\gamma(x) M^*_{\alpha\beta\gamma}(x)$$
$$S^{*(ws)} := -n_\alpha n_\beta n_\gamma M^*_{\alpha\beta\gamma} \tag{23}$$

The semi-integral fields in Eq. (21) include higher order derivatives of primary field variables, which lead to increasing inaccuracy of the solution. To overcome this problem, we decompose the original 4th order governing PDEs into a coupled set of 2nd order PDEs by introducing a new field variable as

$$m^*(x) := \nabla^2 w^*(x), \tag{24}$$

Then, the complet set of governing equations for primary field variables $\left\{w^*, m^*, \psi_0^*\right\}$ is given by Eqs (21) and (24).

3. Numerical implementation

Instead of discretization of the analyzed domain into the mesh of finite elements, as it is done in classical FEM, only the net of nodal points is utilized [11]. Around each node, the field variables are approximated within a finite element that is created automatically according to the position of the reference node in the analyzed domain Ω. If we utilize the bi-quadratic Lagrange element (with 9 nodes), various variants of creation of the moving FE are shown in Figure 1.

The approximation of the spatial variation of a field variable $f \in \left\{w, m, \psi_0\right\}$ is given by polynomial interpolation within the moving finite element E^a as

$$f(\mathrm{x})\big|_{E^a} = \sum_{k=1}^{9} f^{a_k} N^k(\xi), \quad f^{a_k} = f\left(\mathrm{x}^{a_k}\right), \tag{25}$$

where ξ stays for intrinsic coordinates (ξ_1, ξ_2), $N^k(\xi)$ is the shape function in Lagrange finite element [12], and a_k is the global number of the node on element E^a with local number $k \in \{1, 2, \ldots, 9\}$. To account for the second-order derivatives of the field variables, it is necessary to employ finite elements with complete higher-order polynomial interpolation, at least bi-quadratic Lagrange FE defined with 9 nodes.

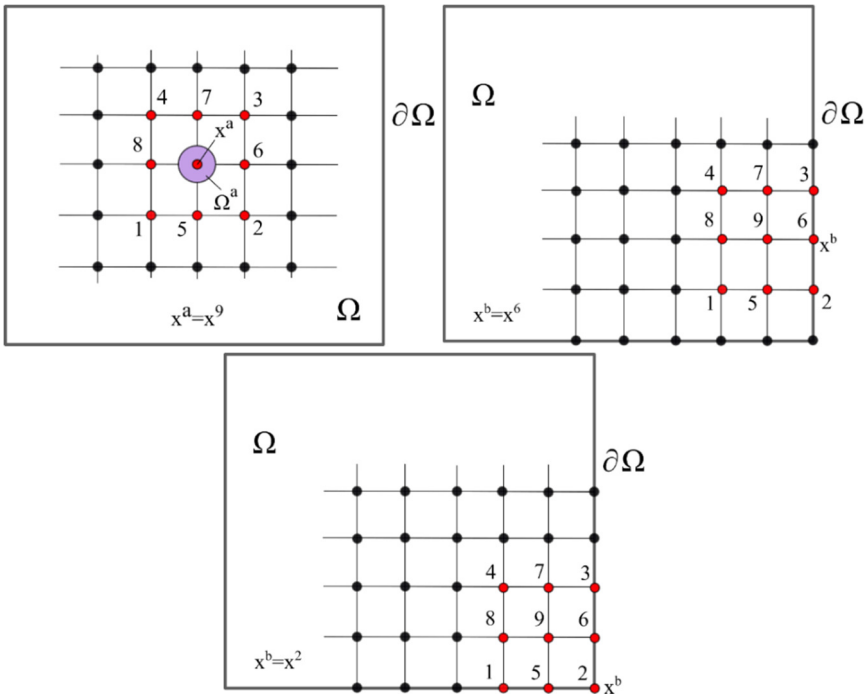

Fig. 1. Scheme of creation of the moving FE around the interior node $\mathbf{x}^a$ as well as the boundary and corner nodes $\mathbf{x}^b$

The 1st and 2nd order derivatives of the field variable can be approximated on the FE as

$$f_{,\beta}(\mathrm{x})\Big|_{E^a} = \left.\frac{\partial f(\mathrm{x})}{\partial x_\beta}\right|_{E^a} = \sum_{k=1}^{9} f^{a}{}_{k} b^{ka}_{\beta}(\xi), \tag{26a}$$

$$f_{,\alpha\beta}(\mathrm{x})\Big|_{E^a} = \left.\frac{\partial^2 f(\mathrm{x})}{\partial x_\alpha \partial x_\beta}\right|_{E^a} = \sum_{k=1}^{9} f^{a}{}_{k} b^{ka}_{\alpha\beta}(\xi), \tag{26b}$$

where $b^{ka}_{\beta}(\xi) = Y^a_{\beta\gamma}\dfrac{\partial N^k(\xi)}{\partial \xi_\gamma}$ and $b^{ka}_{\alpha\beta}(\xi) = Y^a_{\beta\gamma}\left[Y^a_{\lambda\mu} N^k_{,\mu\gamma}(\xi) - Y^a_{\lambda\alpha} J^a_{\alpha\nu,\gamma} b^{ka}_{,\nu}\right]$.

Recall that the matrix $[Ya]$ is the inverse of the Jacobi matrix, i.e. $[Y^a] = [J^a]^{-1}$, and

$$J_{\gamma\lambda} = \left.\frac{\partial x_\gamma}{\partial \xi_\lambda}\right|_{E^a} = \sum_{k=1}^{9} x^{a}_{\lambda}{}_{k} \frac{\partial N^k(\xi)}{\partial \xi_\gamma}. \tag{27}$$

Since the present approach involves no element interfaces, it also avoids the difficulties associated with discontinuities in the derivatives of approximated fields at element boundaries, as in the standard FEM.

4. Numerical experiments

To analyze the problems under consideration through numerical simulation, a square plate geometry was adopted. The plate possesses a dimensionless side length of $L = 1$ and a constant thickness of $h = \mathrm{L}/100$. This domain was discretized using 36 x 36 uniformly distributed nodal points. For the stationary analysis, the plate was subjected to a constant voltage of $\Phi^{\pm} = \Phi_0 \sin(\pi \mathrm{x})$, where $\Phi_0 = 100$ V applied on the top and bottom surfaces, while $q_0 = 0$. Mechanically, all plate edges were considered clamped (CE) and traction-free. Electrically, the edge boundary conditions were evaluated under Dirichlet (DE) conditions $\phi_0^* = 0$. The resulting deflection responses of homogeneous and functionally graded material (FGM) plates under this stationary voltage loading are comparatively presented in the following figures. Both the linear and quadratic variation of material coefficients is assumed.

Figure 2 illustrates the effect of a spatially dependent Young's modulus governed by the power-law function on the plate's deflection. Figure 2a demonstrates that, for a fixed linear exponent ($p = 1$), the increasing level of gradation (ζ) leads to a systematic decrease in the maximum deflection. This outcome is expected, as a higher value of ζ corresponds to a greater overall structural stiffness, thereby enhancing the plate's resistance to bending under the applied electrical load. Figure 2b explores the role of the gradation exponent (p). It is observed that a quadratic gradation results in a larger peak deflection compared to a linear gradation ($p = 1$). This can be attributed to the spatial distribution of stiffness; the quadratic profile renders the plate more compliant in the central region (where bending moments are maximal) and stiffer towards the edges, leading to a greater overall deflection than the linearly stiffening profile.

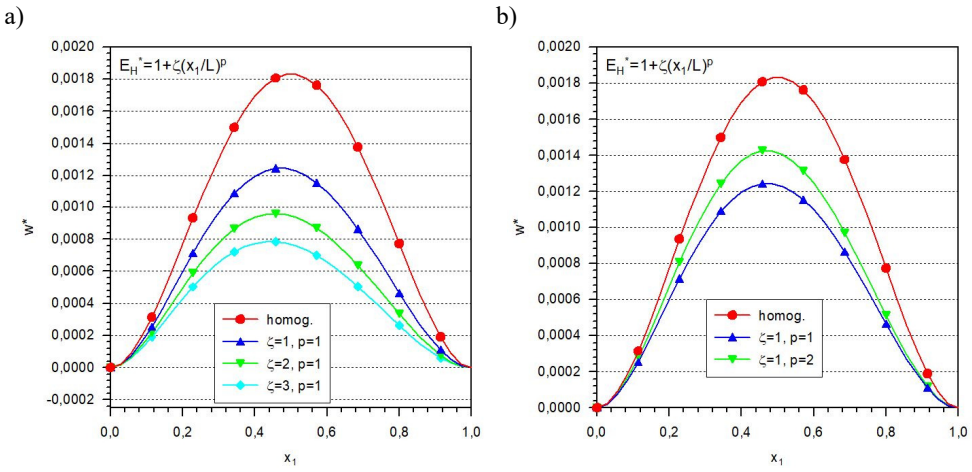

Fig. 2. Comparison of the deflections of the thin micro/nanoplate for various (a) levels (ζ) and (b) exponents (p) of in-plane gradation of Young's modulus

The influence of the gradation of the flexoelectric coefficient is shown in Figure 3. The results show a significant difference in the behaviour of a plate compared to the case with stiffness gradation. As shown in Figure 3a, increasing the level of gradation (ε) results in a substantial increase in the plate's deflection. This highlights the crucial role of the flexoelectric coefficient as the primary driver of electro-mechanical actuation; a higher average coefficient enhances the conversion of electrical energy into mechanical deformation, thus amplifying the bending response. Conversely, Figure 3b reveals that a linear gradation ($r=1$) produces a larger deflection than a quadratic one ($r=2$). This suggests that the bending behaviour is highly sensitive to the spatial distribution of the flexoelectric coupling. A linear increase in the coefficient along the plate's axis appears to align more effectively with the developing strain gradients.

From Figure 4, it is obvious the in-plane gradation has no influence on the bending response of the thin micro/nanoplate.

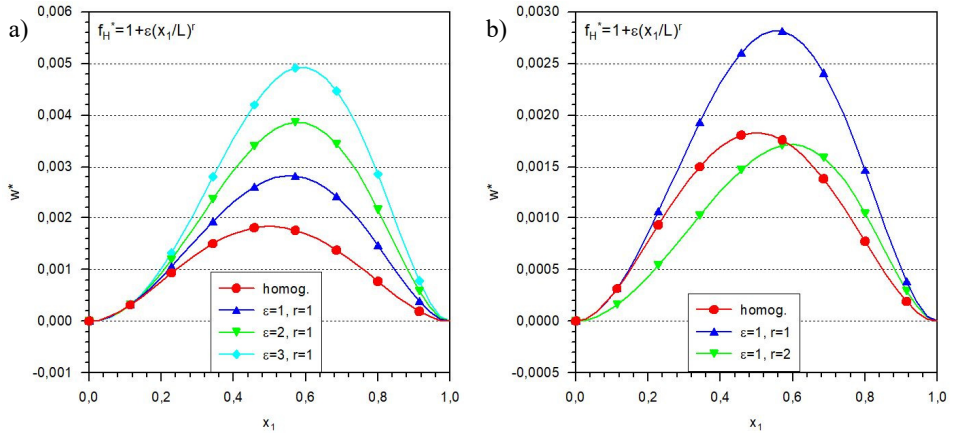

Fig. 3. Comparison of the deflections of the thin micro/nanoplate for various (a) levels (ε) and (b) exponents (r) of in-plane gradation ε and two kinds of gradation of flexoelectric coefficient

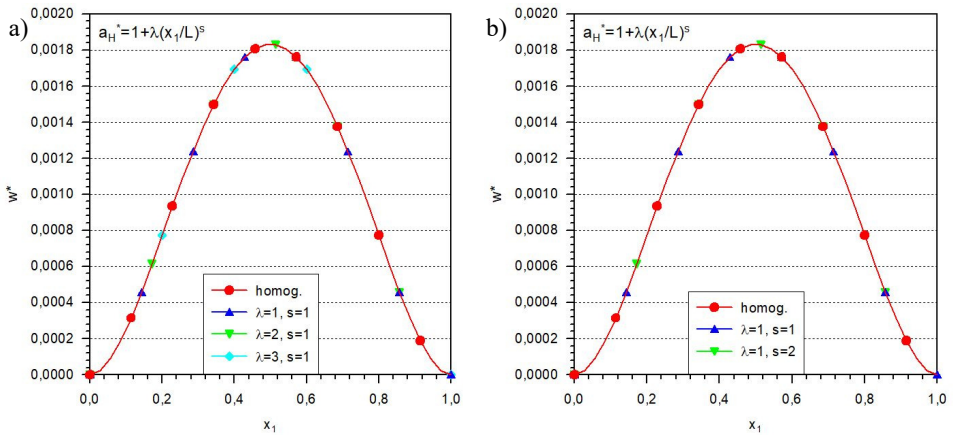

Fig. 4. Comparison of the deflections of the thin micro/nanoplate for various (a) levels (λ) and (b) exponents (s) of in-plane gradation ε and two kinds of gradation of the permittivity coefficient

5. Conclusions

The governing equations have been developed for thin FGM micro/nano plates with flexoelectric effects within the Kirchhoff-Love (KLT) plate bending theory. The in-plane power-law functional gradation of material coefficients is considered. The strong form of governing equations combined with the Moving Finite Element approximation method for the solution of boundary value problems of FGM micro/ nano plates has been developed. Numerical examples have been performed in order to investigate the effects of in-plane gradations of material coefficients within FGM plates subjected to stationary voltage load. From the presented results it is clear the in-plane gradation of material coefficients has a significant effect on the mechanical behaviour of FGM micro/nano plates. The results demonstrate that the in-plane functional gradation provides a versatile methodology for tuning the electromechanical behaviour of flexoelectric nanostructures. Enhancing the flexoelectric coefficient amplifies the bending response, while increasing the stiffness tends to suppress it. Furthermore, the appropriate choice of the gradation exponent offers a powerful tool for optimizing the device performance by strategically tailoring the material property distribution across the domain.

Acknowledgments

The financial support by the Science Grant Agency of the Slovak Republic through the grant VEGA-2/0084/24 is greatly acknowledged.

The authors would like to thank the reviewers for their insightful comments and constructive suggestions. Their expertise and detailed feedback significantly improved the quality and clarity of this manuscript.

References

[1] Li, X., Bhushan, B., Takashima, K., Baek, C.-W., & Kim, Y.-K. (2003). Mechanical characterization of micro/nanoscale structures for MEMS/NEMS applications using nanoindentation techniques. *Ultramicroscopy*, *97*, 481-494.

[2] Ke, L.L., & Wang, Y.S. (2011). Size effect on dynamic stability of functionally graded microbeams based on a modified couple stress theory. *Compos. Struct.*, *93*, 342-350.

[3] Tsiatas, G.C. (2009). A new Kirchhoff plate model based on modified couple stress theory. *Int. J. Solids Struct.*, *46*, 2757-2764.

[4] Lam, D., Yang, F., Chong, A., Wang, J., & Tong, P. (2003). Experiments and theory in strain gradient elasticity. *J. Mech. Phys. Solids*, *51,* 1477-1508.

[5] Sator, L., Sladek, V., Sladek, J., & Young, D. (2016). Elastodynamics of FGM plates by mesh-free method. *Composite Structures*, *140*, 309-322.

[6] Sator, L., Sladek, V., & Sladek, J. (2014). Coupling effects in elastic analysis of FGM composite plates by mesh-free methods. *Compos. Struct*., *115*, 100-110.

[7] Khorshidi, S., Chakouvari, S., Askari, H., & Cveticanin, L. (2022). Free vibrations of flexoelectric FGM conical nanoshells with piezoelectric layers: Modeling and analysis. *Energies*, *15*(9), 2973. DOI: 10.3390/en15092973.

[8] Sharma, S., Kumar, R., Talha, M., Vaish, R. (2021). Flexoelectric poling of functionally graded ferroelectric materials. *Adv. Theory Simul.*, *4*(1), 2000158. DOI: 10.1002/adts.202000158.

[9] Shan, L., Xiao, G., Li, A., Zhou, S., Wang, L., Su, W., Liu, Y., Yang, L., & Song, X. (2025). Nonlinear forced vibration of the FGM piezoelectric microbeam with flexoelectric effect. *Alex. Eng. J.*, *110*, 386-399.

[10] Naskar, S., Shingare, K.B., Mondal, S., & Mukhopadhyay, T. (2022). Flexoelectricity and surface effects on coupled electromechanical responses of graphene reinforced functionally graded nanocomposites: A unified size-dependent semi-analytical framework. *Mech. Syst. Signal Process.*, *169*, 108757. DOI: 10.1016/j.ymssp.2021.108757.

[11] Sladek, V., Repka, M., & Sladek, J. (2019). Moving finite element method. *WIT Trans. Eng. Sci.*, *122*, 119-129.

[12] Hughes, T.J.R. (1987). *The Finite Element Method: Linear Static and Dynamic Finite Element* A*nalysis*. Prentice-Hall Inc.